Contents lists available at ScienceDirect

Digital Chinese Medicine

journal homepage: http://www.keaipublishing.com/dcmed

Shanxiangyuanye (Turpiniae Folium) for diabetic complications: chemical constituents and therapeutic potential

Ruiyao XIONG[a, b], Shuang CHEN[a, b], Zihao DAI[a, b], Limin GONG[a, b*]

a. School of Pharmacy, Hunan University of Chinese Medicine, Changsha, Hunan 410208, China

b. Key Laboratory for Quality Evaluation of Bulk Herbs of Hunan Province, Hunan University of Chinese Medicine, Changsha, Hunan 410208, China

ARTICLE INFO

Article history
Received 01 April 2025
Accepted 17 June 2025
Available online 25 September 2025

Keywords
Shanxiangyuanye (Turpiniae Folium)
Diabetic complications
Anti-glycation
Hypoglycemic
Anti-oxidant

ABSTRACT

Objective To analyze the chemical constituents of Shanxiangyuanye (Turpiniae Folium) through liquid chromatography-tandem mass spectrometry (LC-MS/MS) method, and to evaluate their anti-oxidant, hypoglycemic, and anti-glycation activities related to diabetic complications.

Methods The supernatant of Shanxiangyuanye (Turpiniae Folium) (TFS), obtained following water extraction and alcohol precipitation, was analyzed by LC-MS/MS. Antioxidant activity of TFS *in vitro* was evaluated using three experimental approaches: the 1,1-diphenyl-2-picrylhydrazyl (DPPH) radical scavenging assay, the 2,2'-azino-bis(3-ethylbenzothiazoline-6-sulfonic acid) ($ABTS^+$) radical cation decolorization assay, and the hydroxyl (·OH) radical scavenging assay. To comprehensively evaluate hypoglycemic potential, α-glucosidase inhibition was measured to analyze *in vitro* hypoglycemic activity. Subsequently, *in vitro* models were developed to examine anti-glycation activity through the bovine serum albumin (BSA)-fructose (Fru), BSA-methylglyoxal (MGO), BSA-glyoxal (GO), and D-arginine (Arg)-MGO systems, with particular attention to the inhibitory effects of TFS. Furthermore, the concentrations of fructosamine, protein carbonyls, sulfhydryl groups, and β-amyloid in the glycation solution were quantified using the BSA-Fru model following 7-d of incubation at 37 °C.

Results Using LC-MS/MS analysis in both positive and negative ion modes, we identified 750 chemical components in TFS, primarily including organic acids, amino acids, and their derivatives. *In vitro* activity studies demonstrated that TFS exhibited remarkable free radical scavenging capacity, with half-maximal inhibitory concentrations (IC_{50}) of 0.47, 1.56, and 0.36 mg/mL against DPPH, $ABTS^+$, and ·OH radicals, respectively. Regarding hypoglycemic activity, TFS dose-dependently inhibited α-glucosidase activity (IC_{50} = 0.21 mg/mL), displaying comparable efficacy to the clinical drug acarbose (IC_{50} = 0.23 mg/mL). Notably, TFS intervened in the glycation process: IC_{50} values were 0.22, 1.91 – 4.96, and 4.09 mg/mL in the BSA-Fru, BSA-MGO/GO, and Arg-MGO models, respectively, with the most prominent inhibitory effects observed in the BSA-Fru model. Furthermore, although TFS may not effectively preserve thiol groups in BSA or reduce thiol oxidation during glycation, it significantly reduces fructosamine levels (in a dose-dependent manner), decreases β-amyloid formation, and inhibits protein carbonylation ($P < 0.000\ 1$).

Conclusion The findings demonstrate that TFS exhibits a complex chemical composition with potent antioxidant, hypoglycemic, and anti-glycation activities. These results provide

*Corresponding author: Limin GONG, E-mail: glm5065451@163.com.

Peer review under the responsibility of Hunan University of Chinese Medicine.

DOI: 10.1016/j.dcmed.2025.09.012

Citation: XIONG RY, CHEN S, DAI ZH, et al. Shanxiangyuanye (Turpiniae Folium) for diabetic complications: chemical constituents and therapeutic potential. Digital Chinese Medicine, 2025, 8(3): 413-424.

compelling scientific evidence supporting TFS's potential as a natural adjuvant for diabetes prevention and complication management, while laying a solid foundation for its applications in functional food development and adjunctive antidiabetic therapeutics.

1 Introduction

Type 2 diabetes mellitus (T2DM), accounting for over 90% of all diabetes mellitus (DM) cases, induces multi-organ damage, affecting the eyes, kidneys, heart, blood vessels, and nerves [1]. Epidemiological data indicate that approximately 50% of T2DM patients develop microvascular complications (e.g., nephropathy, retinopathy), while 27% may experience macrovascular complications (e.g., cardiovascular disease). Current management of T2DM in developed countries primarily focuses on glycemic control and cardiovascular risk mitigation [2]. Although pathophysiological mechanisms of diabetes are complex, therapeutic strategies for disease and complication management encompass antioxidant, anti-inflammatory, and anti-glycation approaches, which are crucial for effective diabetes control and delaying diabetic complication progression [1, 3]. The hyperglycemic state promotes non-enzymatic glycation reactions between reducing sugars and proteins/lipids, leading to the information of advanced glycation end products (AGEs). AGEs activate signaling pathways such as nuclear factor (NF)-κB, thereby increasing reactive oxygen species (ROS) synthesis and inducing oxidative stress and chronic inflammation, the core mechanisms underlying diabetic complications [4-6]. Therefore, inhibiting oxidative stress and glycation reactions can effectively delay disease progression while protecting cells and tissues from damage.

Shanxiangyuanye (Turpiniae Folium), derived from *Turpinia arguta* Seem., is a traditional medicinal plant species indigenous to damp, shaded mountain forest regions, primarily distributed across Guangdong, Guangxi, Yunnan, and Guizhou provinces. As a folk remedy of medicinal plant in southern China, its roots and leaves are traditionally recognized for therapeutic properties, including heat clearance, detoxification, sore throat alleviation, anti-swelling effects, and blood circulation promotion to relieve pain. Conventionally, fresh leaves are decocted in water for oral administration to treat tonsillitis, pharyngitis, tracheitis, and to prevent common cold, or crushed for topical application to address skin ulcers, both demonstrating significant therapeutic efficacy [7, 8]. Modern investigations have identified abundant bioactive chemical components in Shanxiangyuanye (Turpiniae Folium), including flavonoids, triterpenoids, and polysaccharides, exhibiting multiple pharmacological effects such as anti-inflammatory, antibacterial, analgesic, and immunomodulatory effects. Notably, its leaves demonstrate α-glucosidase inhibitory activity, providing a scientific basis for potential diabetes treatment [9, 10]. Furthermore, Shanxiangyuanye (Turpiniae Folium) polysaccharides (TFP) and their cotton-like polysaccharide fraction (TFP-1a) show remarkable hypolipidemic effects through mechanisms involving lipid metabolism regulation, oxidative stress and inflammation alleviation, and hepatic pathological improvement. Experimental studies have confirmed the potent free radical scavenging capacity of these polysaccharides and their inhibitory effects on lipopolysaccharide (LPS)-induced inflammatory responses [11, 12]. However, current research has mainly focused on the isolated components (e.g., polysaccharides), while the chemical composition and bioactivities, particularly those related to diabetes treatment—of the water-extracted and alcohol-precipitated supernatant of Shanxiangyuanye (Turpiniae Folium) (TFS) fraction remain inadequately elucidated.

The liquid chromatography-tandem mass spectrometry (LC-MS/MS) method was employed to analyze the TFS components, establishing a foundational basis for examining its biological activity. Subsequently, the potential applications of TFS related to diabetes management and associated complications were assessed, with an emphasis on its antioxidative, hypoglycemic, and anti-glycation properties. The research objective was to investigate the broader medicinal significance of Shanxiangyuanye (Turpiniae Folium), aiming to provide fresh insights and practical guidance for the effective utilization of this resources.

2 Materials and methods

2.1 Materials and chemicals

Shanxiangyuanye (Turpiniae Folium) (Batch No. 20210806) was supplied by Hunan Jiming Pharmaceutical Co., Ltd. (Changsha, China) and authenticated by Dr. Zhi WANG from the School of Pharmacy, Hunan University of Chinese Medicine. The main reagents included aminoguanidine hydrochloride (AG), fructose (Fru), methylglyoxal (MGO), glyoxal (GO), D-arginine (Arg), and 2,4-dinitrophenylhydrazine (purchased from Shanghai Macklin Biochemical Co., Ltd., China), bovine serum albumin (BSA, from Seven Innovation Biotechnology Co., Ltd., China), 1-deoxy-1-morpholino-D-fructose (from Shanghai Yuanye Bio-Technology Co., Ltd., China), nitrotetrazolium blue chloride (NBT), 5,5'-dithiobis (2-nitrobenzoic acid) (DTNB), L-cysteine, and thioflavine T (from Shanghai RYON Biotechnology Co., Ltd., China),

1,1-diphenyl-2-picrylhydrazyl radical (DPPH) [TCI (Shanghai) Chemical Industry Development Co., Ltd., China], and the 2,2'-azino-bis(3-ethylbenzothiazoline-6-sulfonic acid) ($ABTS^+$) total antioxidant capacity assay kit (Beyotime Biotechnology, China). Distilled water was used throughout the experiments, and all other solvents conformed to analytical grade standards.

2.2 Sample preparation and extraction

Shanxiangyuanye (Turpiniae Folium) was subjected to a series of procedures including shearing, drying, crushing, sieving, and weighing. The extraction procedure involved two cycles of ultrasonic-assisted water extraction (500 W, 30 min) at a fixed solid-to-liquid ratio of 1 : 40 g/mL. The combined extracts were concentrated under reduced pressure (– 0.09 MPa, 65 °C) to obtain a concentrated solution. Anhydrous ethanol was then added to achieve a solution with a 75% ethanol volume fraction, followed by static incubation at 4 °C for 24 h. The mixture was then centrifuged at 3 000 rpm for 15 min to separate the supernatant from alcohol-precipitated residues. Ultimately, the supernatant was concentrated under reduced pressure (– 0.09 MPa, 65 °C) and subsequently freeze-dried to yield the supernatant derived from the water extraction-alcohol precipitation of Shanxiangyuanye (Turpiniae Folium) (TFS; yielded 15.6%).

2.3 LC-MS/MS analysis

2.3.1 High-performance liquid chromatography (HPLC) conditions Sample extracts were analyzed using a HPLC system with the following specifications: a Waters ACQUITY UPLC HSS T3 C18 column (1.8 μm, 2.1 mm × 100 mm) was employed. The solvent mixture consisted of water (0.04% acetic acid) and acetonitrile (0.04% acetic acid). The gradient program began at a ratio of 95 : 5 v/v at 0 min, shifted to a 5 : 95 v/v ratio at 11.0 min, maintained at a 5 : 95 v/v ratio until 12.0 min, and then returned to 95 : 5 v/v at 12.1 min. The flow rate was maintained at 0.40 mL/min, with the column temperature set at 40 °C and an injection volume of 2 μL. The effluent was alternately linked to an electrospray ionization-triple quadrupole-linear ion trap (QTRAP)-mass spectrometer (MS) in alternating mode.

2.3.2 Electrospray ionization (ESI)-QTRAP-MS/MS Mass spectrometric analysis was performed using QTRAP system, specifically the API 6 500 QTRAP LC-MS/MS system equipped with ESI Turbo IonSpray interface. Scanning was conducted in both linear ion trap (LIT) and triple quadrupole (QQQ) under the control of Analyst 1.6 software (AB Sciex). The ESI source operated in both positive and negative ion modes with the following parameters: turbo spray ion source, source temperature set at 500 °C, ionspray voltage of 5 500 V, and gas pressure settings for ion source gas I (GSI), gas II (GSII), and curtain gas (CUR) at 55, 60, and 25 psi, respectively. The collision gas (CAD) was maintained at high pressure. Instrument tuning and mass calibration were performed using 10 μmol/L and 100 μmol/L polypropylene glycol solutions in both QQQ and LIT modes. Multiple reaction monitoring (MRM) experiments were acquired in QQQ scans, with nitrogen as the collision gas at 5 psi, and declustering potential (DP) and collision energy (CE) settings were further optimized for each specific MRM transition. A designated series of MRM transitions was observed in alignment with metabolites eluting during the analysis period.

2.3.3 Identification and quantification of metabolites Mass spectral data were processed using software Analyst 1.6.3. Metabolite identification was achieved by analyzing secondary mass spectra while eliminating redundant signals caused by various isotopes, in-source fragmentation, adducts like K^+, Na^+, NH_4^+, and dimerization phenomena. Metabolite information was compiled by comparing accurate mass-to-charge (m/z) ratios values, retention times (RTs), and fragmentation profiles against the Metware Database (MWDB). Metabolite quantification was conducted via MRM mode on a QQQ MS. In MRM mode, the QQQ initially filters precursor ions of the target metabolites, thereby effectively reducing interference from ions of other compounds with identical molecular weights. Then, the QQQ selectively detects distinctive fragment ions generated by precursor ion dissociation within the collision chamber, thus minimizing non-target ion interference and improving quantification precision.

2.4 *In vitro* antioxidant activity assays

2.4.1 DPPH scavenging assay The measurement of antioxidant activity involved evaluating the reduction of DPPH radicals, based on the approach outlined by LONE et al. [13], with minor adjustments. According to preliminary experimental results, various concentrations of samples (0.432, 0.540, 1.080, 2.160, and 4.320 mg/mL) were prepared. In a test tube, 2 mL of the sample solution was added, followed by a DPPH solution of 2 mL (100 μmol/L in methanol) in the sample group. A control group was set up by substituting the sample solution with the solvent, and a blank group was made by replacing the DPPH solution with the solvent. The mixtures were well vortexed and then incubated at room temperature, protected from light, for a duration of 30 min. Afterward, 200 μL of each mixture was transferred to a 96-well microtiter plate, and the absorbance was recorded at 517 nm. The DPPH radical scavenging activity was determined using the following formula:

$$\text{Inhibition}\ (\%) = (A_C - A_S)/A_C \times 100\%$$

where A_C and A_S are the absorbance values of the control and sample, respectively.

2.4.2 ABTS$^+$ radical scavenging activity The antioxidant capacity was evaluated using the rapid ABTS$^+$ radical cation assay. The assay procedure was conducted as follows: the ABTS$^+$ stock solution and oxidant solution were prepared by mixing equal volumes (200 μL each) of ABTS$^+$ stock solution and oxidant solution. Following preparation, the ABTS$^+$ working stock solution was first stored at room temperature in the dark for 12 – 16 h. The prepared ABTS$^+$ working stock solution remained stable for 2 – 3 d, stored at room temperature protected from light. Prior to use, the ABTS$^+$ working stock solution was diluted with phosphate-buffered saline (PBS) to generate the ABTS$^+$ working solution. In a 96-well plate, 200 μL of ABTS$^+$ working solution was mixed with 10 μL of each test sample at various concentrations (0.086 4, 0.108 0, 0.144 0, 0.216 0, 0.270 0, 0.432 0, 0.540 0, and 1.080 0 mg/mL), followed by incubation at room temperature for 6 min. The absorbance was measured at 734 nm, and the ABTS$^+$ radical scavenging activity was calculated using the following formula:

$$\text{ABTS + scavenging effect (\%)} = (A_B - A_A)/A_B \times 100\%$$

where A_B and A_A denote the absorbance values for the blank and the samples under examination, respectively.

2.4.3 Hydroxyl (·OH) radical scavenging activity assay In accordance with the technique detailed by BU et al. [14] with minor modifications, 2 mL of solution samples with varying concentrations were mixed with 2 mL of ferrous sulfate solution (8 mmol/L), 2 mL of salicylic acid solution (8 mmol/L), and 2 mL of hydrogen peroxide solution (8 mmol/L). A control group was set up by replacing the sample solution with 2 mL of distilled water, while a blank control was prepared by replacing the hydrogen peroxide solution with 2 mL of distilled water. The resulting mixtures were then incubated in a water bath at 37 °C for 30 min. Following this, 200 μL of each mixture was taken to measure the absorbance of the reaction system at 536 nm. The ·OH radical scavenging activity was assessed using the following formula:

$$\text{·OH radical scavenging effect (\%)} = (A - A_0)/(A_C - A_0) \times 100\%$$

where A signifies the absorbance of the samples being tested, while A_0 and A_C represent the absorbance values for the blank and control groups, respectively.

2.5 *In vitro* assays for hypoglycemic activity

The α-glucosidase inhibitory activity was evaluated following the protocol outlined by BRICEÑO-ISLAS et al. [15], with minor modifications. In a 96-well microtiter plate, 50 μL of the sample solution was added, along with a blank control consisting of 0.1 mol/L phosphate buffer (pH 6.8) instead of the sample. Next, 100 μL of α-glucosidase (at a concentration of 1 U/mL in 0.1 mol/L phosphate buffer, pH 6.8) was included, and the mixture was incubated at 37 °C for 10 min. After this period, 50 μL of 5 mmol/L p-nitrophenol-α-D-glucopyranoside (pNPG) was introduced, and the incubation at 37 °C continued for another 10 min. The reaction was halted by adding 50 μL of 0.2 mol/L anhydrous sodium carbonate (Na_2CO_3). A positive control group (acarbose) was simultaneously established. Absorbance readings were taken at 405 nm, and the results were reported as the percentage of α-glucosidase inhibition compared to acarbose. The percentage inhibition of α-glucosidase was determined using the following formula:

$$\text{Inhibition (\%)} = (A_0 - A)/A_0 \times 100\%$$

where A_0 indicates the absorbance in the absence of the sample (replaced by distilled water), and A signifies the absorbance in the presence of the tested samples.

2.6 Anti-glycation activity assay

2.6.1 Short-term modeling of BSA-Fru The BSA-Fru short-term model was developed based on the approach of WU et al. [16], with minor modifications. An *in vitro* glycation model using BSA-Fru was utilized to explore the glycation process. A 1.5 mol/L Fru solution and a 60 mg/mL BSA solution were formulated with a 0.2 mol/L phosphate buffer (pH 7.4). In 2 mL tubes, 600 μL of the BSA solution was combined with 600 μL of the Fru solution along with 200 μL of the sample solution (at concentrations of 0.468, 0.936, 1.872, 3.743, and 9.358 mg/mL) for the sample group. This mixture was well mixed and incubated at 50 °C for 24 h. Meanwhile, a positive control group was set up by substituting the sample solution with 200 μL of AG solution (at concentrations of 0.5, 1.0, 1.5, 2.0, and 2.5 mg/mL), and a blank control was created using 200 μL of phosphate buffer (0.2 mol/L, pH 7.4) instead of the sample solution. Furthermore, a sample control was established by using 1 200 μL of 0.2 mol/L phosphate buffer (pH 7.4) in place of the 600 μL BSA solution and 600 μL Fru solution. Fluorescence intensity of the reaction system was assessed using a multifunctional enzyme marker with an excitation wavelength set at 370 nm and an emission wavelength at 440 nm. The rate of inhibition of AGEs was determined using the formula:

$$\text{AGEs inhibition (\%)} = (A_0 - A + A_C)/A_0 \times 100\%$$

where A_0, A, and A_C represent the absorbance values of the blank, sample, and control groups, respectively.

2.6.2 Modeling of BSA-MGO/GO The BSA-MGO/GO models were developed based on the previously reported

methods [17, 18], with minor modifications. These BSA-MGO/GO models were utilized to assess the intermediate phase of protein glycation. Solutions of 60 mmol/L MGO, 60 mmol/L GO, and 30 mg/mL BSA were prepared in 0.2 mol/L phosphate buffer (pH 7.4). In a 2 mL tube, a sequential addition of 600 μL of either MGO or GO solution, 600 μL of the BSA solution, and 200 μL of the sample solution (with concentrations of 0.468, 0.936, 1.872, 3.743, and 9.358 mg/mL) was performed to create the sample group. The resulting mixture was thoroughly agitated and then incubated at 37 °C for 3 d. In parallel, the sample group was incubated with 200 μL of AG solution (at concentrations of 0.5, 1.0, 1.5, 2.0, and 2.5 mg/mL) instead of the sample solution, serving as a positive control. Furthermore, a blank control was prepared using 200 μL of 0.2 mol/L phosphate buffer (pH 7.4) in place of the sample solution, while 1 200 μL of the phosphate buffer (0.2 mol/L, pH 7.4) replaced 600 μL of either MGO or GO solution and the BSA solution to create the sample's internal control. The fluorescence intensity of the reaction system was assessed using a multifunctional enzyme marker, with an excitation wavelength of 370 nm and an emission wavelength of 440 nm. The formula used for calculations was aligned with that of the BSA-Fru model.

2.6.3 Modeling of Arg-MGO The Arg-MGO model was developed based on the approach outlined by SHENG et al. [18], with minor modifications. A 0.2 mol/L phosphate buffer (pH 7.4) was utilized to create an Arg solution with a concentration of 30 mg/mL, alongside an MGO solution at 60 mmol/L. In 2 mL tubes, a mixture was prepared by combining 600 μL of the Arg solution with 200 μL of the sample solution with concentrations of 0.468, 0.936, 1.872, 3.743, and 9.358 mg/mL. This mixture was thoroughly combined and incubated at 37 °C for 2 h. Afterward, 600 μL of MGO solution was incorporated into the sample group, mixed efficiently, and incubated again at 37 °C for 3 d. Furthermore, 200 μL of AG solution at concentrations of 0.5, 1.0, 1.5, 2.0, and 2.5 mg/mL was employed as the positive control, while a blank control consisted of 200 μL of 0.2 mol/L phosphate buffer (pH 7.4). For self-control of the samples, 1 200 μL of phosphate buffer (0.2 mol/L, pH 7.4) was used in place of the 600 μL of Arg and 600 μL of MGO solutions. The fluorescence intensity of the reaction system was assessed using a multifunctional enzyme marker, with an excitation and an emission wavelength of 370 nm and 440 nm. The formula for calculation was aligned with that of the BSA-Fru model.

2.6.4 Long-term modeling of BSA-Fru and its indicators measurement (i) Preparation of glycation solution. The *in vitro* glycation long-term model using BSA-Fru was constructed following the methodology outlined by DENG et al. [19]. A Fru solution with a concentration of 1.5 mol/L and a BSA solution at 60 mg/mL were created using a 0.2 mol/L phosphate buffer (pH 7.4). In 5 mL tubes, we combined 1 800 μL BSA solution, 1 800 μL Fru solution, and 600 μL of various sample solutions (with concentrations of 0.468, 0.936, 1.872, 3.743, and 9.358 mg/mL) to create the sample group solution. This mixture was mixed thoroughly and incubated at 37 °C for a duration of 7 d to achieve the glycation system solution. Simultaneously, AG solutions (with concentrations of 0.5, 1.0, 1.5, 2.0, and 2.5 mg/mL) were prepared to serve as positive controls, while the 0.2 mol/L phosphate buffer (pH 7.4) was utilized as a blank control instead of the sample solution. Additionally, 3 600 μL of phosphate buffer was utilized instead of 1 800 μL of BSA and 1 800 μL of Fru for the sample's own control. Furthermore, an equivalent volume of BSA solution was prepared as the glycation system solution, with all other procedures remaining consistent with those of the sample group. Once the reaction was finished, the solution was taken out and kept at – 20 °C for future analysis.

(ii) Determination of fructosamine content. In accordance with the procedure described by AWASTHI et al. [20], the NBT approach was utilized to measure the fructosamine levels in the glycation model, which serves as an initial product of protein glycation. A 0.5 mmol/L NBT solution was prepared using a 0.1 mol/L carbonate buffer (pH 10.8). Next, a mixture of 20 μL from the glycation system was combined with 180 μL of the NBT solution. Following incubation at 37 °C for 10 min, the absorbance was assessed at 530 nm with a multifunctional enzyme reader. Furthermore, a standard curve was generated using 1-deoxy-1-morpholino-D-fructose as the standard to accurately assess the fructosamine generated in the reaction.

(iii) Determination of protein carbonyl content. The technique employed for assessing protein carbonyl content was based on the method of RAVICHANDRAN et al. [21], with minor modifications. The quantification of protein carbonyls was performed utilizing the 2,4-dinitrophenylhydrazine (DNPH) method. A solution of DNPH at 10 mmol/L was prepared by diluting it in 2.5 mol/L hydrochloric acid. Next, 500 μL of the glycation system was combined thoroughly with the DNPH solution and allowed to react at room temperature for 15 min. After this reaction period, an additional 500 μL of a 20% trichloroacetic acid solution was introduced to precipitate the proteins. The mixture was mixed to ensure complete integration. Following this, another 500 μL of the 20% trichloroacetic acid solution was added to precipitate the proteins. The supernatant was discarded, and the resultant precipitate was washed three times with a mixture of ethanol and ethyl acetate (1 : 1, v/v). To completely dissolve the precipitate, 1 mL of an 8 mol/L urea solution was added, and absorbance was recorded at 370 nm. A molar absorptivity coefficient of 22 000 L/(mol·cm) was

utilized to determine the protein carbonyl content, while the concentration of protein in the glycation system was assessed using a bicinchoninic acid protein assay (BCA) kit. The findings were presented as nmol carbonyl per mg of protein.

(iv) Determination of sulfhydryl content. The measurement of sulfhydryl groups was carried out based on the assay outlined by DENG et al. [19], with necessary modifications. To prepare a 5 mmol/L DTNB solution, a 0.1 mol/L phosphate buffer (pH 7.4) was utilized. Next, a 100 μL of DTNB solution was mixed thoroughly with 100 μL of the glycation system solution and incubated at room temperature for 15 min. The absorbance was subsequently assessed at 410 nm using a multifunctional enzyme reader. At the same time, a standard curve was generated using L-cysteine as the calibration standard to quantify the sulfhydryl groups present in the reaction mixture. Furthermore, the protein concentration in the glycation system solution was evaluated using a BCA kit, and results were recorded as nmol of sulfhydryl groups per mg of protein.

(v) Determination of β-amyloid content. For the assessment of β-amyloid content, a modified technique according to RAVICHANDRAN et al. [21] was employed. A total of 100 μL of the glycation system solution was mixed with 100 μL of a 20 μg/mL thioflavin T solution. The resulting mixture was incubated at 25 °C for 60 min. The fluorescence intensity of the samples was measured at an excitation wavelength of 370 nm and an emission wavelength of 440 nm, with the results presented as β-amyloid fluorescence intensity per 10^6.

2.7 Statistical analysis

Data were analyzed using SPSS 20.0 statistical software, with data expressed as mean ± standard deviation (SD). Statistical differences in the data were analyzed using one-way analysis of variance (ANOVA), and $P < 0.05$ was considered statistically significant.

3 Results

3.1 LC-MS/MS analysis of the TFS chemical constituents

LC-MS/MS analysis identified samples in both positive and negative ion modes (Figure 1A and 1B). A total of 750 compounds, recognized by LC-MS/MS evaluation of TFS, were divided into 22 distinct categories of substances, which mainly included organic acids, amino acids, nucleosides and their derivatives, alkaloids, lipids, sugars, alcohols, flavonoids, and other compounds. The proportion of each compound category is illustrated in Figure 1C, while the details of the top 20 compounds in TFS are listed in Table 1. More comprehensive data are available in Supplementary Table S1. The classification, RTs, molecular weights, ionization modes, ion modes, and compound contents of the various metabolites were also detailed. These findings suggested that the major metabolites in TFS consisted predominantly of organic acids and derivatives, flavonoids, as well as amino acids and their derivatives, comprising the principal constituents of the extract.

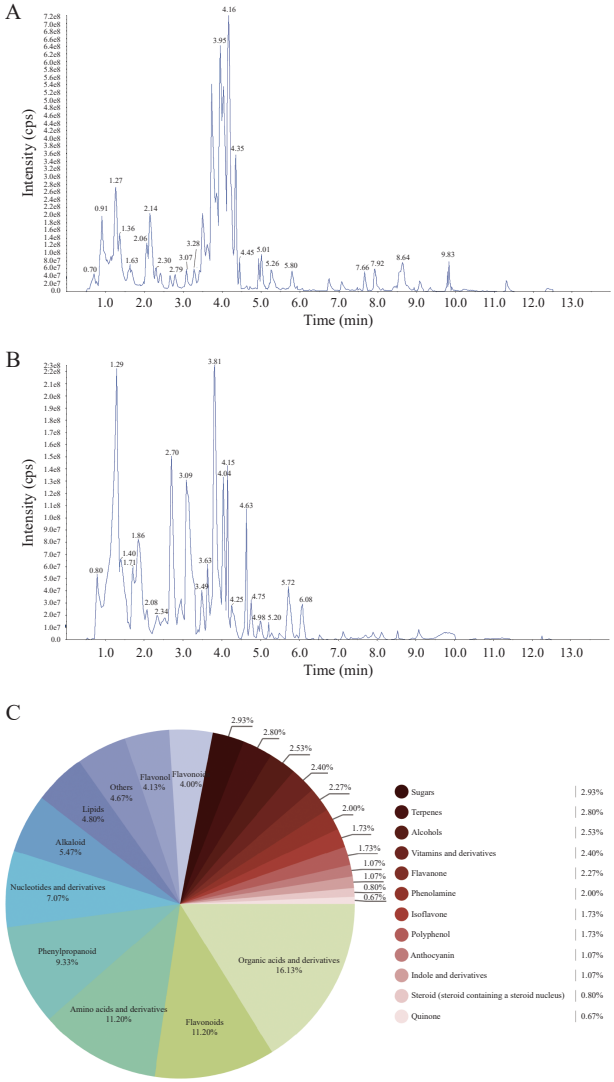

Figure 1 Total ion chromatograms (TIC) obtained from LC-MS/MS under varying ion modes

A, TIC in positive ion mode. B, TIC in negative ion mode. C, classification and percentage of metabolites in TFS.

3.2 Antioxidant activity of TFS with DPPH, $ABTS^+$, and ·OH radical scavenging capacities

DPPH radicals, as the stable free radicals, are widely used for quick and straightforward evaluation of antioxidant properties for natural products [22]. The scavenging activity was observed to increase in a manner dependent on concentration, rising from 0.432 mg/mL to 4.32 mg/mL (Figure 2A). The highest scavenging activity of 92.52% was recorded at a concentration of 4.32 mg/mL. Although the DPPH scavenging activity exhibited a concentration-dependent enhancement, the rate of increment

Table 1 Chemical composition of TFS by LC-MS

No.	Class	Compound	RT (min)	Molecular weight (Da)	Ionization model	Ion mode	Compounds content (%)
1	Flavone	Apigenin 5-O-glucoside	3.81	432.11	[M+H]+	Positive	4.22
2	Flavone	Apigenin 7-rutinoside (isorhoifolin)	4.01	578.16	[M+H]+	Positive	4.00
3	Lipids	14,15-Dehydrocrepenynic acid	8.52	276.22	[M+H]+	Positive	3.92
4	Phenylpropanoids	Brevifolincarboxylic acid	3.02	292.02	[M-H]-	Negative	3.82
5	Amino acid and derivatives	L-Phenylalanine	1.93	165.08	[M+H]+	Positive	3.56
6	Flavone	Apigenin 7-O-neohesperidoside (rhoifolin)	4.01	578.16	[M+H]+	Positive	3.52
7	Phenylpropanoids	Ferulic acid	4.07	194.06	[M-H]-	Negative	3.41
8	Phenylpropanoids	3-Hydroxy-4-methoxycinnamic acid	4.08	194.06	[M-H]-	Negative	3.25
9	Nucleotide and derivatives	Adenosine	1.83	267.10	[M+H]+	Positive	3.00
10	Isoflavone	Genistein 7-O-glucoside (genistin)	4.01	432.11	[M+H]+	Positive	2.43
11	Alkaloids	Choline	0.76	103.10	[M+H]+	Positive	2.33
12	Organic acids and derivatives	Gallic acid	1.74	170.02	[M-H]-	Negative	2.20
13	Organic acids and derivatives	Succinic acid	1.35	118.03	[M-H]-	Negative	2.18
14	Flavone	Apigenin 7-O-glucoside (cosmosiin)	4.21	432.10	[M+H]+	Positive	1.60
15	Flavonol	Kaempferol 3-O-robinobioside (biorobin)	3.76	594.16	[M+H]+	Positive	1.54
16	Alkaloids	Acid orange 20	6.09	350.03	[M]-	Negative	1.49
17	Vitamins and derivatives	Niacinamide	1.52	122.10	[M+H]+	Positive	1.37
18	Others	Vomifoliol	3.97	224.14	[M-H]-	Negative	1.32
19	Organic acids and derivatives	2,4-Dihydroxybenzoic acid	2.75	154.03	[M-H]-	Negative	1.30
20	Sterides	β-Sitosterol	7.75	414.39	[M+H]+	Positive	1.28

gradually diminished at higher concentrations. The half-maximal inhibitory concentration (IC_{50}) value of TFS for DPPH radical scavenging activity was calculated to be 0.47 mg/mL, indicating its notable efficacy in neutralizing DPPH free radicals.

Antioxidants can neutralize $ABTS^+$ radicals by hydrogen atom donation, a process that stabilizes $ABTS^+$ by forming stable molecules [16]. TFS exhibited concentration-dependent radical scavenging activity, increasing from 0.086 4 mg/mL to 1.08 mg/mL, and peaking at 58.54% of 1.08 mg/mL (Figure 2B). The IC_{50} of TFS in scavenging $ABTS^+$ radicals was determined to be 1.56 mg/mL.

·OH radicals, known for their high reactivity, pose a significant threat to living organisms due to their potential to damage adjacent biomolecules, such as DNA, lipids, and proteins [23]. Figure 2C indicates that TFS's ·OH radical scavenging activity displayed a quantitative relationship, with activity increasing concomitantly with concentration. Specifically, scavenging activity rose from 28.19% to 82.92% as the concentration increased from 0.043 2 mg/mL to 0.54 mg/mL. The IC_{50} of TFS in scavenging ·OH radicals was determined to be 0.36 mg/mL.

In summary, TFS exhibits strong antioxidant activity. Notably, its efficacy in scavenging ·OH and DPPH radicals surpasses that of its activity against $ABTS^+$ radicals, a discrepancy potentially attributed to TFS's heightened sensitivity to the former two radicals.

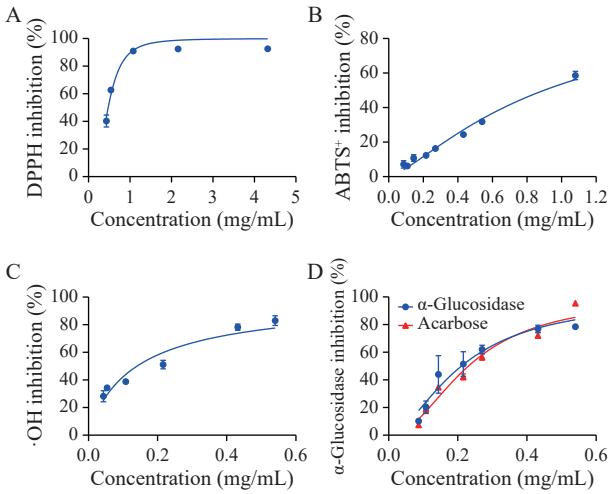

Figure 2 Antioxidant and hypoglycemic activities of TFS

A, the activity of scavenging DPPH radicals. B, the activity of scavenging $ABTS^+$ radicals. C, the activity of scavenging ·OH radicals. D, the inhibitory effects of TFS on α-glucosidase. Data were represented as mean ± SD ($n = 3$).

3.3 Hypoglycemic effects of TFS evaluated by α-glucosidase inhibitory activity

The enzyme α-glucosidase plays a crucial role in carbohydrate digestion and is linked to increased postprandial hyperglycemia levels [1]. Therefore, to assess the

hypoglycemic potential of TFS, its inhibitory activity against α-glucosidase was evaluated. TFS demonstrated a dose-dependent reduction in enzyme activity, with suppression ranging from 10.22% to 78.46% across concentrations of 0.086 4 – 0.54 mg/mL (Figure 2D). The IC_{50} value of TFS was determined to be 0.21 mg/mL, demonstrating comparable efficacy to the positive control acarbose (IC_{50} = 0.23 mg/mL). These findings suggest that TFS exhibits significant hypoglycemic effect, supporting its potential as an antidiabetic agent.

3.4 Characterization of anti-glycation activity in TFS

3.4.1 Effects of TFS on the AGEs inhibition rate in the BSA-Fru model system The BSA-Fru model (representing early-stage glycation) revealed that TFS exhibited significant inhibition of fluorescent AGEs (Figure 3A). This inhibitory effects exhibited a concentration-dependent enhancement within a defined range. As the mass concentration increased from 0.47 mg/mL to 3.74 mg/mL, the inhibition rate of the TFS group rose from 62.33% ± 0.69% to 94.10% ± 3.43%. However, a slight decline in inhibition rate was observed at 9.36 mg/mL, decreasing to 89.67% ± 0.59%. In contrast, the positive control group (AG) exhibited an increase in inhibition rates from 64.00% ± 0.64% to 84.66% ± 1.28% within the concentration range of 0.5 – 2.5 mg/mL. Notably, TFS exhibited weaker inhibition than AG at 0.47 mg/mL but surpassed AG's efficacy at 0.94 mg/mL, achieving peak inhibition of 94.10% ± 3.43% at 3.74 mg/mL. The IC_{50} values for TFS and AG were determined to be 0.22 mg/mL and 0.27 mg/mL, respectively.

3.4.2 Effects of TFS on the AGEs inhibition rate in the BSA-MGO/GO model system The BSA-MGO/GO model, established to replicate intermediate-phase protein glycation, demonstrated that TFS exhibited concentration-dependent inhibition of fluorescent AGEs (Figure 3B and 3C). It was observed that the inhibitory effects of the TFS reaction solution on AGEs exhibited a positive correlation with its mass concentration within a defined range. In the BSA-MGO model, TFS achieved inhibition rates ranging from 21.72% ± 0.32% to 61.11% ± 0.97% across TFS concentrations up to 9.36 mg/mL. In contrast, the positive control group (AG) showed superior inhibition 33.14% ± 0.97% to 67.60% ± 0.32% within the narrower concentration range of 0.5 – 2.5 mg/mL, yielding an IC_{50} value of 1.22 mg/mL. Notably, the BSA-GO model exhibited heightened sensitivity to TFS inhibition. At comparable concentrations, TFS achieved inhibition rates of 31.91% ± 0.49% to 73.79% ± 0.49%, while AG showed 49.00% ± 1.31% to 81.48% ± 0.31% inhibition, culminating in an IC_{50} values of 0.55 mg/mL.

3.4.3 Effects of TFS on AGEs inhibition rate in the Arg-MGO model system Arginine exhibited high vulnerability to modification by MGO, leading to permanent changes in proteins during the advanced phases of glycation. Consequently, the Arg-MGO model serves as an effective approach for evaluating the anti-glycation effects of Shanxiangyuanye (Turpiniae Folium) in inhibiting the MGO binding to arginine [17]. As illustrated in Figure 3D, within a defined concentration range, the TFS reaction solution demonstrated a concentration-dependent inhibitory effect on AGEs formation. The inhibition rate for the sample group increased from 13.65% ± 3.98% to 63.26% ± 2.09% as the TFS concentration rose from 0.47 mg/mL to 9.36 mg/mL, with an IC_{50} value of 4.09 mg/mL. Conversely, the positive control group (AG) showed a comparable concentration-dependent response, with the inhibition rate rising from 32.90% ± 0.33% to 78.11% ± 0.33% across a concentration range of 0.5 – 2.5 mg/mL, similarly yielding an IC_{50} value of 0.94 mg/mL.

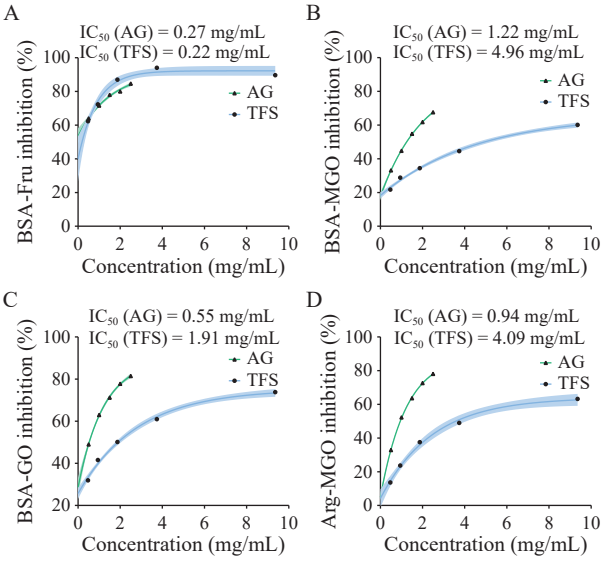

Figure 3 The inhibitory effects of TFS on the formation of AGEs

A, the inhibitory effects on the BSA-Fru model incubated at 50 °C for 24 h. B, the inhibitory effects on the BSA-MGO model incubated at 37 °C for 3 d. C, the inhibitory effects on the BSA-GO model incubated at 37 °C for 3 d. D, the inhibitory effects on the Arg-MGO model incubated at 37 °C for 3 d. Data were represented as mean ± SD (n = 3).

3.4.4 Determination of fructosamine content Fructosamine, formed through the covalent binding of glucose to proteins, acts as a marker for early-stage glycation products. Figure 4A illustrates that the BSA group exhibited a baseline fructosamine level of 1.74 mmol/L. Conversely, the control group, which involved Fru incubation with BSA, demonstrated a notable elevation in fructosamine levels. Interestingly, as the concentration of the TFS sample set increased from 0.468 mg/mL to 3.743 mg/mL, a downward trend in fructosamine levels was observed, reaching a minimum value of 3.743 mg/mL where the fructosamine concentration measured 26.64 mmol/L (P < 0.000 1). These findings indicate that TFS effectively inhibits the formation of early-stage

glycation products like fructosamine, highlighting its importance in managing diabetic complications.

3.4.5 Determination of protein carbonyl content Glycation, a non-enzymatic reaction between proteins and sugars, initiates the formation of unstable Schiff bases and the subsequent production of stable ketamines. This process involves a series of reactions that result in the formation of protein carbonyl compounds [24]. Protein carbonyl compounds, as intermediate products of glycation reactions, facilitated cross-linking between protein molecules and significantly affected their biological functions. Figure 4B illustrates the carbonyl content in the BSA group, the blank control group (glycosylated), and the treated TFS sample group. Notably, the blank control group exhibited a higher protein carbonyl content of 22.89 nmol/mg, whereas the BSA group had a protein carbonyl content of 9.55 nmol/mg. Furthermore, a concentration-dependent effect was observed with varying concentrations of TFS, where the protein carbonyl content decreased from 15.39 nmol/mg to 12.57 nmol/mg as the sample solution concentration increased from 0.468 mg/mL to 9.358 mg/mL (P < 0.000 1). These findings suggest that TFS potentially inhibited the accumulation of protein carbonyl content.

3.4.6 Determination of sulfhydryl content The study indicates that increased oxide generation leads to the loss of protein thiol groups through oxidation, with the extent of protein oxidative damage directly reflected in the reduction of thiol levels [25]. As shown in Figure 4C, the BSA group exhibited a significantly higher thiol content of 111.89 nmol/mg protein compared with 54.45 nmol/mg protein in the glycated blank control group, confirming that the decrease in thiol content reflects BSA oxidation. However, after TFS treatment, the thiol content dropped to 30.68 nmol/mg protein and gradually decreased further with increasing concentrations. These findings suggest that while TFS may not effectively preserve the thiol groups in BSA or reduce thiol oxidation during glycation, it exhibits significant efficacy in other aspects such as antioxidation, hypoglycemic effects, and other modulation of anti-glycation pathways.

3.4.7 Determination of β-amyloid content β-Amyloid can significantly influence the protein physiological activity and demonstrates a strong association with the progression of neurodegenerative diseases and T2DM, as highlighted in the research. Thioflavin T shows the capability to interact with β-amyloid, with the resulting fluorescence intensity exhibiting a positive correlation to the extent of protein cross-linking [26]. In Figure 4D, the blank control group (devoid of any sample) exhibited the maximum β-amyloid content, marked by the peak fluorescence intensity, which was 1.49 times greater than that found in the BSA group, indicating a substantial glycation level in the control group. In contrast, in the TFS group, the fluorescence intensity of amyloid-associated decreased from 67.67 × 10^6 to 26.00 × 10^6 as TFS concentrations escalated from 0.468 mg/mL to 9.358 mg/mL (P < 0.000 1), thereby illustrating TFS's effective inhibition of protein cross-linking.

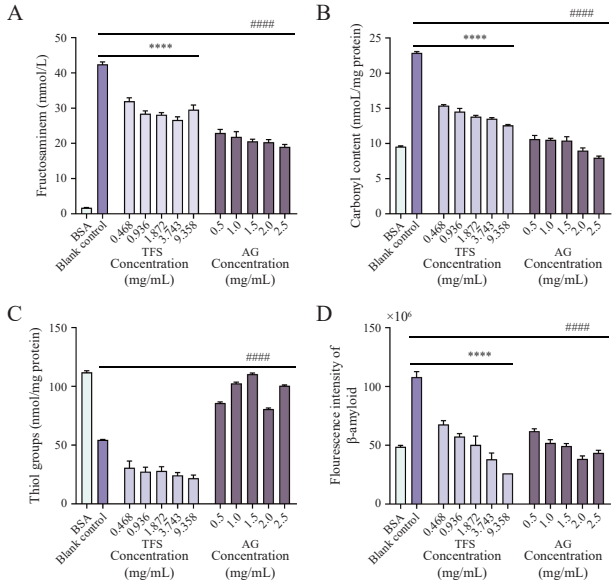

Figure 4 Assessment of the anti-glycation activity of TFS

A, the level of fructosamine. B, the amount of carbonyls. C, the quantity of thiol groups. D, the fluorescence intensity of β-amyloid. Data were represented as mean ± SD (n = 3). $^{****}P$ < 0.000 1, the TFS group compared with the blank control group. $^{####}P$ < 0.000 1, the AG group compared with the blank control group

4 Discussion

Through LC-MS/MS analysis in both positive and negative ion modes, 750 compounds were identified in TFS, primarily including flavonoids, organic acids, amino acid derivatives, phenylpropanoids, and terpenoids, which may serve as the material basis for its biological activities. Literature reports indicate that flavonoids exhibit antioxidant and hypoglycemic properties. The high content of apigenin glycosides (e.g., apigenin-5-O-glucoside, 4.22%) correlates with the potent free radical scavenging ability of TFS and α-glucosidase inhibitory activity, while organic acids and amino acids may synergistically enhance these effects [27, 28]. Phenylpropanoids, such as ferulic acid, have been reported to effectively scavenge hydrogen peroxide, peroxynitrite, and superoxide radicals [29]. Terpenoids like ursolic acid exhibit significant antioxidant activity, likely mediated through free radical scavenging mechanisms [30, 31], consistent with the observed structure-activity relationships in this study. The results demonstrated that TFS exhibited remarkable antioxidant activity, with IC_{50} values of 0.47, 1.56, and 0.36 mg/mL against DPPH, $ABTS^+$, and ·OH radicals, respectively, indicating its potential to mitigate oxidative damage. Its α-glucosidase inhibitory activity (IC_{50} = 0.21 mg/mL) is

comparable to that of the clinical hypoglycemic drug acarbose (IC_{50} = 0.23 mg/mL), suggesting its potential as a natural adjuvant for blood sugar control. Therefore, these findings collectively suggest that TFS possesses both antioxidant and hypoglycemic properties.

The samples' anti-glycation capacity is generally evaluated using the BSA-Fru glycation model [32]. Given that Fru metabolites (e.g., MGO and GO) exhibit high reactivity and preferentially bind to protein amino groups (particularly arginine ureido groups), thereby promoting protein cross-linking and the formation of AGEs [33, 34], inhibiting glycation reactions and their oxidative derivatives may offer novel strategies for diabetic complication prevention and treatment. This study reveals that TFS can modulate both oxidative stress and the glycation pathway—two key pathological mechanisms in diabetic complications. TFS showed significant inhibitory effects across multiple glycation models (BSA-Fru, BSA-MGO/GO, and Arg-MGO), with maximal inhibition observed in the BSA-Fru model (IC_{50} = 0.27 mg/mL). Notably, at elevated concentrations, its anti-glycation efficacy (e.g., 94.10% inhibition in the BSA-Fru model) even surpassed that of the positive control drug aminoguanidine (AG). A slight reduction in inhibitory activity was observed at 9.36 mg/mL. Additionally, TFS significantly decreased fructosamine levels and protein carbonyl content (P < 0.000 1), indicative of intervention in early-to-middle glycation stages. Its inhibitory effects on β-amyloid formation (P < 0.000 1) further suggest a role in preventing protein cross-linking, a key feature of diabetic neuropathy. This dual-action mechanism positions TFS as a promising natural agent for addressing the multifactorial nature of diabetic complications, highlighting the medicinal value of Shanxiangyuanye (Turpiniae Folium) in diabetes drug development.

Although this study elucidates the potential of TFS, further *in vivo* validation remains essential. These findings yield critical insights into the antidiabetic mechanisms of Shanxiangyuanye (Turpiniae Folium) and offer a scientific foundation for its development as a functional food or pharmaceutical agent endowed with antioxidant and hypoglycemic properties.

5 Conclusion

The findings demonstrate that TFS exhibits significant antioxidant, hypoglycemic, and anti-glycation activities, primarily attributed to its rich composition of flavonoids, organic acids, and amino acid derivatives. Notably, TFS manifests potent free radical scavenging capabilities and α-glucosidase inhibitory effects comparable to those of the clinical drug acarbose. Furthermore, TFS effectively modulates multiple stages of the glycation cascade, reducing fructosamine levels, protein carbonyl content, and β-amyloid formation, thereby highlighting its potential as a dual-targeting agent that simultaneously mitigates oxidative stress and glycation pathways in diabetic complications. These results provide a scientific foundation for developing TFS as a natural therapeutic agent or functional food adjunct for diabetes management.

Fundings

Key Project of Hunan Provincial Education Bureau (23A0307), and Natural Science Foundation of Hunan Province (2025JJ80089).

Competing interests

The authors declared no conflict of interest.

References

[1] FANG YC, DAI W, CAO YH. Study on the correlation of skin advanced glycation end products with diabetic cardiovascular autonomic neuropathy. Diabetes, Metabolic Syndrome and Obesity, 2025, 18: 335–343.

[2] YAN H, ZHOU Q, WANG YQ, et al. Associations between cardiometabolic indices and the risk of diabetic kidney disease in patients with type 2 diabetes. Cardiovascular Diabetology, 2024, 23(1): 142.

[3] KHALID M, PETROIANU G, ADEM A. Advanced glycation end products and diabetes mellitus: mechanisms and perspectives. Biomolecules, 2022, 12(4): 542.

[4] SADEGHI M, MIROLIAEI M, KAMYABIAMINEH A, et al. The impact of AGEs on human health and the development of their inhibitors based on natural compounds. Arabian Journal of Chemistry, 2023, 16(10): 105143.

[5] CHEN YC, MENG ZH, LI Y, et al. Advanced glycation end products and reactive oxygen species: uncovering the potential role of ferroptosis in diabetic complications. Molecular Medicine, 2024, 30(1): 141.

[6] KATEEL R, KASHYAP NN, REDDY SK, et al. Chronic β-carotene, magnesium, and zinc supplementation together with metformin attenuates diabetes-related complications in aged rats. Clinical Nutrition, 2025, 50: 183–197.

[7] Committee for the Chinese Materia Medica. Chinese Herbal Medicine Vol. 5. Shanghai: Shanghai Science and Technology Press, 1999.

[8] XIONG WP. Study on optimization of extraction process of total flavonoids from Turpiniae Folium and *in vitro* antibacterial activity. Feed Research, 2025, 48(5): 107–114.

[9] ZHAO LJ, XIA OX, LIN LM, et al. Optimization of ultrasound-assisted enzymatic polysaccharide extraction from turpiniae folium based on response surface methodology. Digital Chinese Medicine, 2018, 1(3): 239–246.

[10] BONIFACE PK, ELIZABETH FI. Flavones as a privileged scaffold in drug discovery: current developments. Current Organic Synthesis, 2019, 16(7): 968–1001.

[11] YAN J, ZHAO LJ, LI YM, et al. Preparation and characterization

of polysaccharides from Turpiniae Folium and its antioxidative, anti-inflammatory activities and antiproliferative effect on VSMCs. Chemistry & Biodiversity, 2022, 19(11): e202200459.

[12] YANG XL, LI L, ZHANG TF, et al. GC-MS-based serum metabolomic investigations on the ameliorative effects of polysaccharide from Turpiniae Folium in hyperlipidemia rats. Oxidative Medicine and Cellular Longevity, 2021, 2021: 9180635.

[13] LONE S, NARAYAN S, HUSSAIN K, et al. Investigating the antioxidant and anticancer potential of *Daucus* spp. extracts against human prostate cancer cell line C4-2, and lung cancer cell line A549. Journal of Ethnopharmacology, 2025, 337(Pt 2): 118855.

[14] BU YK, YIN BF, QIU ZC, et al. Structural characterization and antioxidant activities of polysaccharides extracted from *Polygonati rhizoma pomace*. Food Chemistry, 2024, 23: 101778.

[15] BRICEÑO-ISLAS G, MOJICA L, URÍAS-SILVAS JE. Functional *Chia* (*Salvia hispanica* L.) co-product protein hydrolysate: an analysis of biochemical, antidiabetic, antioxidant potential and physicochemical properties. Food Chemistry, 2024, 460(Pt 1): 140406.

[16] WU HW, SHU LP, LIANG T, et al. Extraction optimization, physicochemical property, antioxidant activity, and α-glucosidase inhibitory effect of polysaccharides from lotus seedpods. Journal of the Science of Food and Agriculture, 2022, 102(10): 4065–4078.

[17] SHEN YX, XU ZM, SHENG ZW. Ability of resveratrol to inhibit advanced glycation end product formation and carbohydrate-hydrolyzing enzyme activity, and to conjugate methylglyoxal. Food Chemistry, 2017, 216: 153–160.

[18] SHENG ZW, AI BL, ZHENG LL, et al. Inhibitory activities of kaempferol, galangin, carnosic acid and polydatin against glycation and α-amylase and α-glucosidase enzymes. International Journal of Food Science & Technology, 2018, 53(3): 755–766.

[19] DENG YJ, LIU Y, ZHANG CH, et al. Characterization of enzymatic modified soluble dietary fiber from *Rhodomyrtus tomentosa* fruits: a potential ingredient in reducing AGEs accumulation. Food and Bioprocess Technology, 2023, 16(1): 232–246.

[20] AWASTHI S, PREETHY R, SARASWATHI NT. Nordihydroguaiaretic acid prevents glycation induced structural alterations and aggregation of albumin. International Journal of Biological Macromolecules, 2019, 122: 479–484.

[21] RAVICHANDRAN G, LAKSHMANAN DK, MURUGESAN S, et al. Attenuation of protein glycation by functional polyphenolics of dragon fruit (*Hylocereus polyrhizus*); an *in vitro* and *in silico* evaluation. Food Research International, 2021, 140: 110081.

[22] DOU ZM, CHEN C, HUANG Q, et al. Comparative study on the effect of extraction solvent on the physicochemical properties and bioactivity of blackberry fruit polysaccharides. International Journal of Biological Macromolecules, 2021, 183: 1548–1559.

[23] SU Y, LI L. Structural characterization and antioxidant activity of polysaccharide from four auriculariales. Carbohydrate Polymers, 2020, 229: 115407.

[24] KHAN MS, REHMAN MT, ISMAEL MA, et al. Bioflavonoid (hesperidin) restrains protein oxidation and advanced glycation end product formation by targeting AGEs and glycolytic enzymes. Cell Biochemistry and Biophysics, 2021, 79(4): 833–844.

[25] BALU M, SANGEETHA P, MURALI G, et al. Age-related oxidative protein damages in central nervous system of rats: modulatory role of grape seed extract. International Journal of Developmental Neuroscience, 2005, 23(6): 501–507.

[26] ZHANG QZ, HUANG ZJ, WANG Y, et al. Chinese bayberry (*Myrica rubra*) phenolics mitigated protein glycoxidation and formation of advanced glycation end-products: a mechanistic investigation. Food Chemistry, 2021, 361: 130102.

[27] OUAHABI S, DAOUDI NE, LOUKILI EH, et al. Investigation into the phytochemical composition, antioxidant properties, and *in-vitro* anti-diabetic efficacy of *Ulva lactuca* extracts. Marine Drugs, 2024, 22(6): 240.

[28] ZHANG B, XIA T, DUAN WH, et al. Effects of organic acids, amino acids and phenolic compounds on antioxidant characteristic of Zhenjiang aromatic vinegar. Molecules, 2019, 24(20): 3799.

[29] ZHANG ZE, YAO SD, LIN WZ, et al. Mechanism of reaction of nitrogen dioxide radical with hydroxycinnamic acid derivatives: a pulse radiolysis study. Free Radical Research, 1998, 29(1): 13–16.

[30] SHI YJ, LENG YF, LIU DS, et al. Research advances in protective effects of ursolic acid and oleanolic acid against gastrointestinal diseases. The American Journal of Chinese Medicine, 2021, 49(2): 413–435.

[31] NOR FM, MOHAMED S, IDRIS NA, et al. Antioxidative properties of *Pandanus amaryllifolius* leaf extracts in accelerated oxidation and deep frying studies. Food Chemistry, 2008, 110(2): 319–327.

[32] ZHANG L, LU Y, YE YH, et al. Insights into the mechanism of quercetin against BSA-fructose glycation by spectroscopy and high-resolution mass spectrometry: effect on physicochemical properties. Journal of Agricultural and Food Chemistry, 2019, 67(1): 236–246.

[33] ZHAO L, ZHU XL, YU Y, et al. Comprehensive analysis of the anti-glycation effect of peanut skin extract. Food Chemistry, 2021, 362: 130169.

[34] MUÑIZ-RAMIREZ A, PEREZ RM, GARCIA E, et al. Antidiabetic activity of *Aloe vera* leaves. Evidence-Based Complementary and Alternative Medicine, 2020, 2020: 6371201.

山香圆叶治疗糖尿病并发症的化学成分及治疗潜力

熊瑞瑶[a, b], 陈双[a, b], 戴子豪[a, b], 龚力民[a, b*]

a. 湖南中医药大学药学院, 湖南长沙 410208, 中国
b. 湖南中医药大学湘产大宗药材品质评价湖南省重点实验室, 湖南长沙 410208, 中国

【摘要】目的 采用液相色谱-串联质谱（LC-MS/MS）技术分析山香圆叶的化学成分，并评价其与糖尿病并发症相关的抗氧化、降糖及抗糖基化活性。**方法** 对山香圆叶经水提醇沉后所得的上清液（TFS）进行 LC-MS/MS 分析。通过三种实验方法评价 TFS 的体外抗氧化活性：1,1-二苯基-2-苦基肼（DPPH）自由基清除实验、2,2′-联氮-双-3-乙基苯并噻唑啉-6-磺酸（$ABTS^{+}$）自由基阳离子脱色实验和羟基（·OH）自由基清除实验；通过 α-葡萄糖苷酶抑制实验分析其体外降糖潜力；随后建立牛血清白蛋白（BSA）-果糖（Fru）、BSA-丙酮醛（MGO）、BSA-乙二醛（GO）及 D-精氨酸（Arg）-MGO 四种体外模型研究其抗糖基化活性来重点观察 TFS 的抑制效果。此外，采用 BSA-Fru 模型在 37 °C 孵育 7 天后，对糖基化溶液中的果糖胺、蛋白质羰基、巯基及 β-淀粉样蛋白的含量进行定量分析。**结果** 通过正、负离子模式下的 LC-MS/MS 分析，从 TFS 中鉴定出 750 种化学成分，主要包括有机酸、氨基酸及其衍生物。体外活性研究表明，TFS 表现出显著的自由基清除能力，对 DPPH、$ABTS^{+}$和·OH 自由基的半抑制浓度（IC_{50}）分别为 0.47、1.56 和 0.36 mg/mL。在降糖活性方面，TFS 以剂量依赖方式抑制 α-葡萄糖苷酶活性（IC_{50} = 0.21 mg/mL），效果与临床药物阿卡波糖相当（IC_{50} = 0.23 mg/mL）。值得注意的是，TFS 可干预糖基化过程：在 BSA-Fru、BSA-MGO/GO 和 Arg-MGO 模型中的 IC_{50} 值分别为 0.22、1.91 – 4.96 和 4.09 mg/mL，其中在 BSA-Fru 模型中抑制效果最为突出。此外，尽管 TFS 在糖化过程中可能无法有效保护 BSA 中的巯基或减少巯基氧化，但能显著降低果糖胺水平（呈剂量依赖性）、减少 β-淀粉样蛋白的形成并抑制蛋白质羰基化（$P < 0.000\,1$）。**结论** 本研究结果表明，TFS 化学成分复杂，具有显著的抗氧化、降糖和抗糖基化活性，为其作为预防糖尿病及并发症的天然辅助剂提供了科学依据，并在功能食品开发和辅助抗糖尿病治疗中奠定了坚实基础。

【关键词】山香圆叶；糖尿病并发症；抗糖基化；降血糖；抗氧化剂